

# Biodegradable, Elastomeric Coatings with Controlled Anti-proliferative Agent Release for Magnesium-based Cardiovascular Stents

Xinzhu Gu <sup>a,b</sup>, Zhongwei Mao <sup>a,c</sup>, Sang-Ho Ye <sup>a,b</sup>, Youngmi Koo <sup>d</sup>, Yeoheung Yun <sup>d</sup>, Tiasha  
Tarannum <sup>e</sup>, Vesselin Shanov <sup>e</sup>, William R. Wagner <sup>a,b,f,g,\*</sup>

<sup>a</sup> McGowan Institute for Regenerative Medicine, University of Pittsburgh, Pittsburgh, PA 15219,  
USA

<sup>b</sup> Department of Surgery, University of Pittsburgh, Pittsburgh, PA 15219, USA

<sup>c</sup> School of Medicine, Tsinghua University, Beijing 100084, China.

<sup>d</sup> National Science Foundation Engineering Research Center for Revolutionizing Metallic  
Biomaterials, North Carolina A & T State University, Greensboro, NC 27411, USA

<sup>e</sup> College of Engineering and Applied Science, University of Cincinnati, Cincinnati, OH 45221,  
USA

<sup>f</sup> Department of Chemical Engineering, University of Pittsburgh, Pittsburgh, PA 15219, USA

<sup>g</sup> Department of Bioengineering, University of Pittsburgh, Pittsburgh, PA 15219, USA

\* Corresponding author. Tel.: +1 412 624 5324; fax: +1 412 624 5363.

E-mail address: [wagnerwr@upmc.edu](mailto:wagnerwr@upmc.edu) (W.R. Wagner)

## **Abstract**

Vascular stent design continues to evolve to further improve the efficacy and minimize the risks associated with these devices. Drug-eluting coatings have been widely adopted and, more recently, biodegradable stents have been the focus of extensive evaluation. In this report, biodegradable elastomeric polyurethanes were synthesized and applied as drug-eluting coatings for a relatively new class of degradable vascular stents based on Mg. The dynamic degradation behavior, hemocompatibility and drug release were investigated for poly(carbonate urethane) urea (PCUU) and poly(ester urethane) urea (PEUU) coated magnesium alloy (AZ31) stents. Poly(lactic-co-glycolic acid) (PLGA) coated and bare stents were employed as control groups. The PCUU coating effectively slowed the Mg alloy corrosion in dynamic degradation testing compared to PEUU-coated, PLGA-coated and bare Mg alloy stents. This was confirmed by electron microscopy, energy-dispersive x-ray spectroscopy and magnesium ion release experiments. PCUU-coating of AZ31 was also associated with significantly reduced platelet adhesion in acute blood contact testing. Rat vascular smooth muscle cell (rSMC) proliferation was successfully inhibited when paclitaxel was released from pre-loaded PCUU coatings. The corrosion retardation, low thrombogenicity, drug loading capacity, and high elasticity make PCUU an attractive option for drug eluting coating on biodegradable metallic cardiovascular stents.

## 1. Introduction

The treatment of occlusive vascular disease has been revolutionized by the implementation of endovascular stents since their introduction in the 1980s. In particular, the advent of drug eluting stents (DES), made from non-degradable metallic frames with polymer coatings, has markedly reduced the incidence of restenosis, precipitated by the overproliferation of vascular wall smooth muscle cells (SMCs). However, the permanent polymers/metals of these devices can cause dysfunctional endothelialization, and a hypersensitivity reaction, which contributes to vascular occlusion due to late stent thrombosis and very late stent thrombosis.[1, 2]

To overcome these limitations, efforts have been devoted to develop biodegradable stents, amongst which degradable metals, such as magnesium and its alloys, are promising for their initial mechanical properties and non-toxic degradation products.[3] However, an obstacle to applying many magnesium-based materials clinically is an oxidation rate that is considered too rapid to allow for optimal vascular remodeling. Many methods have been developed to enhance the corrosion resistance of magnesium alloys through surface modification, such as micro-arc oxidation,[4] plasma anodization[5] and polymer coating.[6-9] Amongst these options, polymer coating is attractive in that in addition to corrosion resistance,[10] the coating can serve as a drug reservoir,[11] and also has the ability to be functionalized with a variety of biomolecules. Specifically, Poly(lactic-co-glycolic acid) (PLGA) and poly(l-lactide) acid (PLLA) have been employed as magnesium alloy stent coatings,[12] although these materials can be moderately thrombogenic, [13-15] and the acidic products from their degradation may stimulate a greater inflammatory response within the vessel wall once the stent is encapsulated by vascular tissue.[16-18] Moreover, due to the very high strains experienced by a stent during dilatation balloon inflation, the poor extensibility of these coating materials might subject the polymer coating to rupture and detachment.[19]

The objective of this study was to develop degradable and elastomeric polymer coatings applicable to blood-contacting, magnesium-based devices. The polymer coating would not only improve corrosion resistance and enhance the thromboresistance in acute blood contact, but also offer controlled release of bioactive agents to inhibit vascular hyperplasia. Poly(ester urethane)urea (PEUU) and poly(carbonate urethane)urea (PCUU), which demonstrate elastomeric behavior and which degrade at differing rates in vivo, have been synthesized and reported previously.[20] These materials are cytocompatible, and have been fabricated as biodegradable elastic patches and applied as temporary mechanical supports to positively alter the remodeling process following myocardial infarction.[21] It was expected that PCUU, which exhibits a slower degradation rate, would increase the corrosion resistance of the underlying magnesium-based substrate. Further, the elastomeric mechanical properties of this family of polymers were expected to be attractive for application as stent coatings since they may be resistant to delamination or fracture during stent expansion by balloon inflation. The effect of control PLGA, PEUU and PCUU polymer coatings on Mg alloy stents was examined in terms of their influence on degradation behavior and acute thrombogenicity. A conventional antiproliferative drug, paclitaxel, was incorporated into the polymers and the bioactivity of the releasate was evaluated by quantifying its effect on SMC proliferation in vitro.

## **2. Experimental Section**

### **2.1 Materials**

#### **2.1.1 Polymer synthesis**

PEUU and PCUU were synthesized from soft segments of polycaprolactone diols (PCL,  $M_n = 2000$ , Sigma Aldrich) and poly(hexamethylene carbonate) diols (PHC,  $M_n = 2000$ , Sigma Aldrich) respectively, and 1, 4-diisocyanatobutane (Sigma Aldrich) hard segment with chain extension by

1,4-diaminobutane (Sigma Aldrich) according to previous reports.[20, 22] PCL or PHC diols, diisocyanatobutane, and diamine were combined in a 1:2:1 molar ratio. Detailed polymer characteristics, including mechanical properties, cytocompatibility, and in vitro and in vivo degradation, have been reported previously.[20] PLGA (50:50 LA:GA) with an average molecular weight of 200,000 g/mol was purchased from Polysciotech and used as received.

### **2.1.2 Preparation of magnesium alloy plates and photochemically etched magnesium stent**

Mg alloy (AZ31, 3% Al, 1% Zn) plate was purchased from Goodfellow Corp. Samples with dimensions of  $10 \times 10 \times 0.25$  mm were used for in vitro degradation tests and blood contacting tests, and samples with dimensions of  $10 \times 5 \times 0.25$  mm were used for primary rat smooth muscle cell (rSMC) growth experiments. The magnesium alloy was progressively polished with a series of silicone carbide sand papers from 400 to 1200 grit.

A photochemically etched stent made of AZ31 alloy with a diameter of 3 mm and a length of 10 mm was studied in previous report.[23] In brief, the stent was fabricated by photochemical etching a 250  $\mu$ m thick foil made of AZ31 alloy. This approach included photolithography to transfer a pattern on the foil, followed by chemical etching. The resulting etched foil had a desired pattern that was determined by the optical photo mask. The etched foil was rolled to form a cylinder and laser welding was used to complete the stent manufacturing.[24] Both AZ31 plates and AZ31 stents were cleaned by sonication with acetone and trichloroethylene and dried under vacuum at room temperature. Stents with a diameter of 4 mm and a length of 13 mm were used for stent expansion tests, and stents with a diameter of 3 mm and a length of 10 mm were used for in vitro degradation tests and blood contacting tests.

### **2.1.3 Polymer coating preparation**

Polymer coatings were created by a dip-coating method. Polymers were dissolved in 1,1,1,6,6,6-hexafluoroisopropanol (HFIP, Oakwood, Inc.) to obtain a 2% (w/v) solution. Then the cleaned

magnesium alloy substrates were dipped into the polymer solution and dried in flowing air for 5 min. The above process was repeated three times. The specimens were further dried in a fume hood overnight and stored in a vacuum desiccator at room temperature. Polymer coated AZ31 plates and uncoated plates were all sterilized by 70% ethanol incubation for 15 min followed by DI water immediately prior to degradation testing, cell culture or blood contact.

#### **2.1.4 Stent inflation**

Polymer coated stents were expanded to 6 mm in diameter using an Abbott Vascular Viatrac® 14 plus peripheral dilation catheter. Stents before and after expansion were sputter-coated with gold/palladium prior to scanning electron microscopy (SEM; JSM-6330F, JEOL USA)

#### **2.2. In vitro degradation tests**

Polymer coating degradation and magnesium alloy substrate corrosion behavior were assessed up to 28 days by analyzing surface morphologies, the release of magnesium ions and the surface atomic compositions after incubation in a degradation medium. This medium was prepared from Dulbecco's modified eagle's medium (DMEM) supplemented with 10% fetal bovine serum (FBS), 1% penicillin/streptomycin (P/S), and 100 U/mL lipase solution from *Thermomyces lanuginosus* to mimic the enzymatically-driven degradation that would occur in vivo. Each sample was vertically inserted into a Falcon® round-bottom tube and immersed in 3 mL degradation medium at 37°C followed by placement of the tube on a hematology mixer (Fisher Scientific) to achieve rocking and fluid transport over the test surfaces. The medium was changed every other day. The release of dissolved magnesium ions from the samples was measured at different time points using inductively coupled plasma atomic emission spectroscopy (ICP-AES, iCAP duo 6500 Thermo Fisher). Three samples were tested for each group. The magnesium concentration for non-contacted degradation medium was subtracted from all data points. The surface of each recovered sample was rinsed, air dried and sputter-coated prior to scanning electron microscopy. The surface

composition following 21 days of degradation testing was studied by energy-dispersive X-ray spectroscopy (EDX, EDX Genesis, EDAX Inc.).

Degradation testing for stents was performed using a fabricated vascular bioreactor designed to simulate the flow conditions found physiologically.[23] The system consisted of a reservoir, pump and flow channel incorporating a conduit section into which the stent could be inserted. Silicon tubing with an inner diameter of 3.2 mm was used as the flow channel. The tubing and reservoir were sterilized for 15 min at 121°C before perfusion of the degradation solution. The stent was not observed to migrate in the flow path. The total volume of the test medium was 300 mL and the pH was  $7.40 \pm 0.05$ . The lengths from pump to sample and from sample to reservoir were both 1 m. The sample was located in the middle of sample channel. This system was located in an incubator where laminar flow at 17 mL/min was implemented. Dynamic testing was performed for 3 days. 3D images of the metallic samples were acquired using a micro-CT (Phoenix Nanotom-M<sup>TM</sup>, GE Sensing & Inspection Technologies GmbH, Germany). The 3D structure provided morphological evidence of the corrosion status before and after dynamic testing of control and polymer-coated stents.

### **2.3. In vitro blood contacting test**

Whole ovine blood was collected by following previously described protocols.[25] NIH guidelines for the care and use of laboratory animals were followed, and all animal procedures were approved by the Institutional Animal Care and Use Committee (IACUC) at the University of Pittsburgh. S-Monovette® tubes (3 mL; Sarstedt, Germany) containing sodium citrate were used to collect the blood. Thrombotic deposition on bare and polymer-coated AZ31 surfaces was assessed in vitro with rocking. Each specimen was placed into a Vacutainer tube (Becton-Dickinson) filled with 4 mL fresh, citrated ovine blood and incubated for 2 h at 37°C on a hematology mixer. After ovine blood contact, surfaces were rinsed 10 times with PBS and treated with 2.5% glutaraldehyde

solution for 2 h at 4°C to fix the platelets deposited on the surface, and then immersed in 1% (w/v) OsO<sub>4</sub> for 1 h. The samples were then serially dehydrated by increasing ethanol solutions from 30% to 100%. The surface was then sputter-coated and observed by SEM. Deposited platelets on each surface were also quantified by a lactate dehydrogenase (LDH) assay with an LDH Cytotoxicity Detection Kit (Clontech Laboratories, Inc. Mountain View, CA).[26] Five separate samples were used for each group.

#### **2.4. Rat Vascular Smooth Muscle Cell Growth**

Polymer films loaded with paclitaxel (Taxol, LC Laboratories, Inc.) were cast from Taxol/polymer/solvent mixture, where Taxol was loaded as 5 wt% to polymer. Polymer films with an average weight of 6 mg were cut from paclitaxel-loaded films and then immersed in 5 mL release medium of PBS buffer with 0.1% (v/v) Tween 20 and 0.1% (v/v) ethanol at pH=7.4 and kept in a 37°C incubator shaker and agitated at 75 rpm. A standard curve was obtained from a series of known concentrations of paclitaxel and the solubility of amorphous paclitaxel was determined to be 15 µg/mL in the buffer solution. At each defined time point, the 5 mL releasate solution was collected and 5 mL of fresh solution was added. The sampling frequencies used were sufficiently high to maintain all the release solutions below the solubility limit and to keep the solutions under sink conditions. Three separate samples were tested for each polymer type. The paclitaxel in the collected releasate was detected at 227 nm using a plate reader (Perkin-Elmer UV/vis Lambda 40, U.S.A.).

Polymer coatings loaded with paclitaxel were prepared by solubilizing Taxol (5 wt % to polymer) into the polymer/solvent mixture prior to dip-coating. Polymer coated and uncoated AZ31 plates were sterilized under UV irradiation for 30 min, then immersed into a well (24-well cell culture plate), followed by seeding with 10<sup>4</sup> cells per well of rSMCs with 1 mL of DMEM supplemented with 10% FBS and 1% P/S solution. After being incubated for 3 h to allow cell attachment, the



specimens were then transferred into new wells and cultured for 7 days. The cell culture medium was exchanged every 3 days. Pieces of tissue culture polystyrene (TCPS) with the same dimension (i.e.  $10 \times 5 \times 0.25$  mm) served as the positive control group. The metabolic activity of rSMCs was measured using a MTS assay kit (Promega CellTiter 96 Cell Proliferation Assay) (n=4). To qualitatively verify the results of the MTS assay, cells were also observed under fluorescence microscopy after live/dead staining with a live/dead viability/cytotoxicity kit (Invitrogen Inc.), and images were taken using fluorescence microscopy (Eclipse Ti, Nikon).

## **2.5. Statistical Analyses**

The data were analyzed by one-way ANOVA with Turkey's test applied for specific comparisons.  $P < 0.05$  was considered to represent a significant difference. All results were presented as the mean  $\pm$  standard deviation.

## **3. Results**

### **3.1. Polymer coating morphology**

Representative surface and cross-section morphologies of the coated and uncoated AZ31 plates were studied by SEM. The surface of polymer coated samples was clean and smooth after coating (**Fig. S1a**). The thickness of the polymer coating was about 10  $\mu\text{m}$ , as indicated from SEM cross-sectional images (**Fig. S1b**). PCUU coated and PLGA coated AZ31 stents were expanded from 4 to 6 mm in diameter using a balloon catheter, with an expansion ratio of 50% (**Fig. S2**). PCUU coating maintained its integrity after expansion, while there were fractures and delamination apparent for the PLGA coating (**Fig. S3**).

### **3.2. In vitro degradation tests**

#### **3.2.1. Polymer coated AZ31 plates**

Surface morphologies for each type of sample at different degradation intervals are shown in **Fig. 1**. After 7 days of corrosion, a network of surface cracks was present on the uncoated alloy, characteristic of magnesium corrosion morphology. This morphology persisted over 14 and 28 days. For polymer coated AZ31 plates, PLGA showed the most aggressive progression of degradation, with formation of a microporous structure at day 7, typical of bulk degradation of a PLGA film.[27, 28] After day 14, the PLGA coating was partially gone, and magnesium alloy substrate was exposed with a cracking morphology similar to the uncoated substrate. After 28 days, the magnesium alloy substrate was more fully exposed to the medium, with what appear to be some residual fragments from the polymer coating. After 7 days, the bulk of PEUU coating was still present on the substrate, although some cracks were found on the polymeric surface and magnesium alloy appeared to be corroding underneath. The cracks on the polymer surface became larger and denser after 14 days. Some parts of polymer coating were gone and the residual polymer film started wrinkling, with a larger area of alloy substrate exposed to the medium at the final time point. For PCUU coatings, at 7 days in medium, the coatings showed the appearance of blebs on the surface, possibly evidence of the formation of gas bubbles at the metal interface. As the incubation time progressed, these bubbles did not appear to grow and the polymer coatings remained intact in most areas.

To further evaluate the degradation of bare and polymer-coated AZ31 plates, ICP-AES was used to determine ionic concentrations of magnesium in the medium collected. All samples showed magnesium ion release from day 2 (**Fig. 2**). PCUU coated magnesium alloy plates showed significantly less ion release than the other three groups for subsequent time points until day 14, beyond which the magnesium ion concentration release was not significantly different between the groups.

**Fig. 3** shows the chemical composition of each uncoated or polymer coated surface after rocking tests in medium for 21 days as detected by EDX analysis. The predominant atoms on the AZ31 surface were Mg, C, and O. The signals of carbon and oxygen indicated the presence of organic components on the surface. The signals for P, together with Mg and O suggest the presence of tertiary magnesium phosphate.[29] Compared with the bare AZ31 sample, the PLGA, PEUU, and PCUU coated substrates showed significantly less surface Mg. PEUU and PCUU coated surfaces exhibited significantly less magnesium element than PLGA coated ones, in agreement with the morphological evidence of **Fig. 1**. The same trend was also observed for aluminum, of which AZ31 contains 3%. The principle components of PLGA, PEUU and PCUU are carbon and oxygen, and the weight percentages of both C and O of polymer coated surfaces were all higher than uncoated ones, which further confirmed the existence of the polymer coating layer.

### **3.2.2. Dynamic degradation of polymer coated AZ31 stents**

**Fig. 4** shows the morphological alterations in uncoated and coated AZ31 stents in the perfusion bioreactor under a wall shear stress of 0.07 Pa for 3 days. Under rocking conditions, the majority of AZ31 plates presented a relatively smooth surface. In contrast, under stronger flow conditions, the AZ31 stent exhibited focal regions of marked mass loss and general coverage with a corrosion product layer. Some stent struts were distorted during the corrosion study, likely due to decreased mechanical strength after degradation and mass loss. There was blebbing observed across the PLGA-coated stents, again, possibly due to hydrogen gas release during the stent corrosion. Wrinkles and cracks were also observed on the coating surface. The PEUU coating layer had a network of 100  $\mu\text{m}$ -scale cracks covering the surface, in some cases exposing small areas of underlying AZ31. For the PCUU coated stent, although one crack was observed on the edge of a stent strut, there was generally a smooth and intact surface structure.

Micro-CT was utilized to study the corrosion morphology of magnesium-alloy stents beneath the polymer coating layers (**Fig. 5**). Macroscopic 3-D corrosion morphologies of AZ31 stents in the vascular bioreactor under a wall shear stress value of 0.07 Pa showed that the uncoated stent struts were notably thinner compared with the other three coated groups, indicating substantial material removal during perfusion tests. Some large and deep corrosion pits appeared on the uncoated sample. Some corrosion pits were found on the surface of the PLGA and PEUU coated stents, and PCUU-coated stents maintained a smooth and homogeneous surface.

### **3.3. In vitro ovine blood contact**

SEM images of uncoated and polymer-coated magnesium alloy plates following 2-hour ovine blood contact qualitatively demonstrated reduced thrombus formation on polymer coated magnesium alloy surfaces (**Fig. 6a**). On the bare AZ31 surface, thrombotic deposition that appeared to involve fibrin formation and red cell entrapment was consistently observed. Also the morphology of the AZ31 surface appeared to be similar to that in the earlier degradation tests (**Fig. 1**). On the PLGA coated surface, small platelet aggregates and a large number of individual platelets with pseudopodia extensions were observed across the surface. In addition, cracking and localized delamination of the PLGA coating were observed. On PEUU coated surfaces, there were fewer deposited platelets and aggregates and these appeared to occur in distinct regions. Only sparse platelets were deposited on the PCUU-coated surface and these generally did not appear to have extended pseudopodia. Platelet deposition on the different surfaces as quantified using the LDH assay (**Fig. 6b**) confirmed the SEM observations with the PLGA coated surface showing significantly greater deposition than PEUU and PCUU coated surfaces. The p-value for the mean comparison between PCUU and PEUU surfaces was on the borderline of the standard set for accepting significance ( $p=0.054$ ).

To better evaluate the hemocompatibility of Mg-based stents, ovine blood contact tests were conducted on AZ31 stents with or without polymer coatings (**Fig. 7**). Thrombi spanning stent struts were observed on the uncoated stent with fibrin deposition. Cracks were present on the edge of the PLGA-coated stents, and platelets aggregates were observed on the surface. Individual platelets were deposited on the PCUU-coated stent surface with pseudopodia extensions. PEUU-coated stents were not evaluated.

### **3.4. rSMC growth**

All polymer films showed sustained paclitaxel release in PBS buffer with 0.1% (v/v) Tween 20 and 0.1% (v/v) ethanol at 37°C for 44 days (**Fig. S4**). For the whole release measurement period, the amount of Taxol released from PEUU was significantly higher than for PCUU and PLGA. A two-stage release profile was observed for PLGA, whereas PEUU and PCUU showed more rapid release in the initial stage than PLGA.

The antiproliferative activity of paclitaxel released from PCUU film coatings was investigated by seeding rSMCs onto PCUU-coated or bare AZ31 plates. Cells were also seeded on free-standing polymer cast films to compare cell adhesion and proliferation on these polymer films versus those cast upon an AZ31 substrate (**Fig. 8a**). After 1 d culture, rSMCs attachment was similar across the different surfaces evaluated. Without paclitaxel present, rSMCs on PCUU films and coatings showed substantial cell proliferation and became confluent by day 7. However, when seeding on polymer films or polymer coatings containing paclitaxel, rSMC numbers did not appear to increase. The formation of gas bubbles under the polymer coating did not appear to affect the location and the manner in which the cells grew, although the coatings became more uneven, making microscope focusing more challenging. Improved cell proliferation was observed on PCUU coated substrates versus the bare AZ31 alloy. Live/dead staining indicated no apparent cellular death on any of the surfaces, whether paclitaxel was present or not.

In support of the above visual observations, the MTS assay of cellular mitochondrial activity, showed similar differences between the surfaces (**Fig. 8b**). rSMCs on surfaces without paclitaxel release showed increased metabolic indices after 3 and 7 d culture, in contrast to cells seeded on films or coatings with paclitaxel release. On those latter surfaces, the metabolic index did not increase further at days 3 or 7, consistent with the lower cell numbers visualized. The metabolic index of rSMCs seeded on PCUU films or coatings showed a comparable increase to that found with the positive control, TCPS.

#### **4. Discussion**

The elution of anti-proliferative pharmaceutical agents from biostable or biodegradable polymer films on metallic stents has been a strategy that has dramatically reduced the clinical incidence of restenosis by inhibiting smooth muscle cell proliferation relative to bare metal stents. Among the current commercially available drug-eluting stents, a paclitaxel eluting TAXUS stent (Boston Scientific, USA), which incorporates a stainless steel platform with a permanent polymer coating polystyrene-b-isobutylene-b-styrene, was approved for clinical trial by FDA in 2004.[30] The zotarolimus eluting Endeavor stent (Medtronic, USA), which is a CoCr platform covered with a permanent phosphorylcholine polymer, and Abbott's XIENCE V™ everolimus drug eluting stent (CoCr platform with a non-erodible acrylic and fluorinated polymers) were approved for clinical treatment of coronary artery disease from FDA later in 2008.[31]

Synthetic biodegradable polymers, such as polylactide (PLA) and PLGA have been investigated for stent coating purposes. These polymers typically undergo ester bond cleavage to form degradation products such as lactic acid and glycolic acid, which can then be cleared from the body. Most reported biodegradable polymer coated drug-eluting stents, such as BioMatrix (Biosensors Int, California), Infinnium (Sahajanand, India), LUC-Chopin2™ (Balton, Poland), EucaTax (Eucatech AG, Germany), are comprised of nondegradable metallic stents and

biodegradable polymer coatings, such as PLA, PLGA, or PLA-co-PCL, and have been approved for clinical trials in some countries.[32] Most recently, Boston Scientific's Synergy drug-eluting stent was approved by the FDA in the US as the first (partially) bioabsorbable stent.[33] The device is comprised of a permanent platinum chromium alloy body coated with everolimus-loaded PLGA.

Although the above-mentioned drug eluting stents represent a major medical advance in the treatment of coronary lesions, since a non-degradable metallic surface is ultimately revealed, the risk for thrombosis and inflammation at later stages centered on this material remain. The treated arterial segment also remains "caged" with a permanent metallic scaffold that can limit options for subsequent interventions. These limitations have supported the ongoing interest in developing fully biodegradable metallic or polymeric stents, because conceptually, once they are fully absorbed, only the remodeled vessels are left behind with no residual prosthesis and therefore no potential adverse interactions with the vessels.[34]

Two biodegradable polymeric stents are worth noting. A PLLA stent (Igaki-Tamai, Japan) received CE Mark approval in 2007 and is used in nine European Union countries to treat peripheral arterial disease. It has a low restenosis rate at 6 months, but also requires high pressure deployment with heated contrast and routine anticoagulant treatment to decrease the thrombotic risk.[35] A bioresorbable PLLA scaffold coated with bioresorbable poly(D,L-lactide) coating/everolimus layer has been developed by Abbott (ABSORB) and has experienced a reduced restenosis ratio compared with bare-polymer stents in clinical trials. It showed positive one-year clinical results and appears to be on track to become the first fully bioabsorbable stent to gain US FDA approval.[36]

Compared with biodegradable polymer stents, there are fewer metallic biodegradable stents in clinical trials. Currently the only biodegradable metal stents in clinical trials is the drug-eluting

absorbable metal stent (DREAMS, Biotronik),[12] which is fabricated from bioabsorbable magnesium alloy with a degradable polymeric coating, (PLGA or, more recently, PLLA). An anti-proliferative agent, (paclitaxel or, more recently, sirolimus) is embedded within the polymer coating. Compared to bioresorbable PLLA stents, DREAMS has benefits related to the improved material properties of a metallic versus a polymer for an intravascular scaffold, specifically: strong radial support, low acute recoil, improved deliverability and high compliance.[37] Additionally, the magnesium is absorbed within 12 months, which is faster than polymer-based bioresorbable scaffolds (2 yrs). Recently the BIOSOLVE-II clinical trial confirmed the safety and effectiveness of DREAMS for treating coronary artery disease, as demonstrated by a low incidence of stent thrombosis and improved lumen loss 6 months following implantation.[38] Among other potential degradable metallic stents, there has been little progress with other candidate metals such as iron, where iron-based stents remain in pre-clinical testing, partly due to stability in the physiological environment resulting in long-term retention.[39] Moreover, iron was observed to generate a layered corrosion product with minimal tissue integration after 9 months in vivo.[40] More recently, zinc has emerged as a candidate degradable metal for stents, with potential ability to reduce restenosis after stent implantation. [41, 42]

With respect to candidate coatings for newly developed magnesium-based stents, it has recently been shown that some biodegradable polymer coatings, e.g. PLA, PLGA, and PCL, did not effectively slow the corrosion rate, and this was attributed to the acidic products generated upon polymer degradation destabilizing the  $Mg(OH)_2$  passivation layer.[10, 43] In the current study, it was found that both PEUU and PCUU provided better protection to the underlying magnesium-based substrate than PLGA. The highly polar urea groups in the polyurethane ureas provide enhanced hydrogen bonding in the hard segments, which act as strong physical crosslinkers. The high molecular weight, the low crystallinity, and the low glass transition temperatures ( $T_g < -46^\circ C$ ) impart good elastomeric mechanical properties to the solid polyurethane coatings.[20] PLGA



typically has a  $T_g$  in the range of 40-60°C, above the physiological temperature of 37°C, and hence the material is glassy and rigid in nature.[44] As a metallic coating, the glassy properties of PLGA may make it susceptible to delamination or fracture, not only when the underlying stent undergoes deformation, such as with crimping or expansion with a balloon catheter, but also during Mg corrosion, as hydrogen gas produced could distend and damage the coating layer. The elastomeric polyurethanes appear to better withstand the force exerted by stent expansion and hydrogen gas generation. Compared to PEUU, it was shown that PCUU maintained a smoother surface in degradation studies and further slowed the corrosion of the underlying magnesium substrate. This effect was attributed to the relatively slower hydrolysis rate of the carbonate versus ester bond.[20, 21] Acidic degradation products (i.e. carboxylic acids) generated upon ester bond degradation, which may damage the  $Mg(OH)_2$  layer, could be a factor in the faster corrosion under PEUU. For carbonate cleavage, the unstable weak acidic degradation products would be expected to quickly decompose into neutral products, (alcohol and carbon dioxide), which would not affect the magnesium corrosion rate.

Magnesium alloy corrosion is affected by the composition of the contacting solution. Various solutions, such as deionized water,[45] PBS,[46] Hank's balanced salt solution,[47] simulated body fluid (SBF),[48, 49] and DMEM[8] have been used to investigate the corrosion behavior of Mg alloys under consideration for physiological settings. Compared to other corrosion solutions, cell growth medium such as DMEM, captures more of the complexity of physiological fluids.[50] In this study, we also added fetal bovine serum and lipase, to better approximate the blood plasma environment and to accelerate degradation of the polymeric coatings. It has been reported that magnesium alloy corrosion slows substantially in the presence of proteins, with adsorbed proteins forming a corrosion-protective layer on the surface of magnesium alloy.[51] In addition to the composition of the degradation medium, fluid dynamics also affect the degradation kinetics, an effect particularly important for vascular stent applications. Both increased local mass transfer and

mechanical forces at the fluid-metal interface accelerate degradation compared to static conditions.[23] This was confirmed in the present study as the majority of the AZ31 plates presented a relatively smooth surface under gentle rocking conditions, while the dynamic flow resulted in severely corroded AZ31 stents with some corrosion product layers facing the flow being embolized, and the mechanical deformation of weakened stent struts (**Fig. 4**).

For blood contacting applications, the hemocompatibility is a primary concern. Alloying has been found to be an effective method of decreasing hemolysis and platelet deposition compared to the pure magnesium controls.[52] Surface-treatment by micro-arc oxidation has also shown significantly decreased hemolysis and greater thromboresistance compared to untreated Mg alloy controls.[53] Surfaces modified with zwitterionic phosphorylcholine or sulfobetaine silanating agents also experienced decreased platelet adhesion compared with control AZ31 surfaces in vitro.[25] Both PEUU and PCUU had significantly reduced platelet deposition relative to uncoated or PLGA coated AZ31, which suggests improved thromboresistance in vivo, at least acutely. There was, however, some platelet deposition observed on both polyurethane surfaces. It has previously been reported that the blood biocompatibility of similar degradable polyurethanes can be improved by grafting phosphorylcholine onto the polymer backbone.[54, 55] This family of polyurethanes showed less platelet deposition compared to PEUU and PCUU; however, their high hydrophilicity and fast degradation rate might possibly lower their anti-corrosion efficacy on Mg-based substrates.

All the polymer films in this study showed sustained Taxol release in PBS/Tween20/ethanol solution (**Fig. S4**).The slower observed initial release from the PLGA film was attributed to its much higher  $T_g$  than PEUU and PCUU. The temperature of the paclitaxel release experiments was 37°C, below the  $T_g$  of PLGA. Therefore, the molecular motion and free volume of the amorphous polymer were limited, thus in turn inhibiting the drug release from the bulk polymer. The later

increase in the drug release for the PLGA film may have been due to a decreased  $T_g$  and hydrolysis of the bulk material.[56] The slower release of paclitaxel from the PCUU compared to PEUU was attributed to its slower degradation rate. rSMC proliferation was successfully inhibited in the presence of paclitaxel, confirming the bioactivity of paclitaxel after solvent contact.

Several limitations in this study should be noted. First, the stent expansion ratio investigated here (50%) is relatively low and was a limit associated with the underlying metal ductility and the employed stent design. Higher strains would need to be investigated using specific Mg-alloy stent designs capable of greater deformations. Further, we did not evaluate the impact of a strained overlying polymer on the inhibition of corrosion behavior. After distension, it is possible that the elastomer barrier properties may be altered and lead to greater corrosion than that found in unstrained stents. Certainly if cracks were to form in the coating at stent locations that experience high levels of deformation, as observed on the PLGA coating at 50% expansion (**Fig. S3**), such defects in the coating would be expected to become sites of highly localized corrosion. Next, the polymer coatings serving as a magnesium corrosion barrier would be expected to only be effective for a limited period, as ultimately it is desired for both coating and stent to be degraded. This study only evaluated processes in the earliest stages for blood contact, and did not carry the degradation or corrosion studies to an advanced state. Such extended studies would be better suited for in vivo testing where a fully functional immune system and ongoing blood flow and mechanical loading would be provided. Moreover, for all of the polymer coatings examined in this report, polymer degradation and underlying metal corrosion ultimately lead to deformation or delamination of the coating from the alloy surface. If this detachment and degradation occurs after incorporation into the vascular wall, it may be of no consequence. However, the employment of a coating that exhibits only surface-erosion may be advantageous to better control alloy corrosion and provide stable drug delivery. Wang et. al. have demonstrated a surface eroding coating, poly(1,3-trimethylene carbonate), that can effectively protect the corrosion of underlying magnesium

substrate with good hemocompatibility and histocompatibility.[10] However, it is not possible to control the degradation rate of this polymer for different applications. With respect to the clinical experience to date with drug eluting coatings, concerns regarding late (>1 year) stent thrombosis due to delayed endothelialization have been problematic.[57] Anti-proliferative drugs, such as paclitaxel and sirolimus, not only limit the proliferation of SMCs, but also endothelial cells, and thus impair the wound healing response.[58] Coating of stents with substances that potentially facilitate endothelial healing may represent a promising therapeutic approach. Many efforts have been devoted to modify the stent surface for guiding the surrounding endothelial cells onto stents, such as the adsorption of peptides,[59] and the immobilization of anti-CD34 antibodies,[60] vascular endothelial growth factor (VEGF),[61] and nitride oxide[62]. A combination of “prohealing” substances (such as VEGF) with established “anti-restenosis” drugs (such as paclitaxel) may represent an interesting approach to obtain the benefit of reduced restenosis by promoting endothelialization while inhibiting SMC proliferation through the sequential release of the two agents.[63]

## **5. Conclusions**

Biodegradable, elastomeric polyurethanes were successfully applied as coatings for magnesium alloy stents in this study. PCUU-coated magnesium stents exhibited improved corrosion resistance in vitro and reduced thrombotic deposition versus uncoated stents or those coated with PLGA. Release of the antiproliferative agent paclitaxel from the PCUU coating was shown to effectively inhibit rSMC proliferation. These results suggest that this biodegradable poly(carbonate urethane)urea might be an attractive material to use as a drug-eluting coating for biodegradable magnesium vascular stents as well as other magnesium devices being developed for applications where extended blood contact would occur.

## Acknowledgements

We gratefully acknowledge the financial support of the National Science Foundation (ERC-RMB, Award NSF 0812348). We also thank Prof. Prashant N. Kumta (Univ. of Pittsburgh) for access to ICP-AES and Dr. Da-Tren Chou for the help with the ICP-AES and EDX experiments. We would also like to thank Dr. Venkat Shankarraman, Mr. Joseph Hanke, and Mr. Teri Horgan who obtained the fresh ovine blood used in this study.

## References

- [1] J.P. Chen, D. Hou, L. Pendyala, J.A. Goudevenos, N.G. Kounis, *JACC Cardiovasc. Interv.* , 2 (2009) 583.
- [2] G.G. Stefanini, B. Kalesan, P.W. Serruys, D. Heg, P. Buszman, A. Linke, T. Ischinger, V. Klauss, F. Eberli, W. Wijns, *Lancet*, 378 (2011) 1940.
- [3] F. Witte, *Acta Biomater.*, 6 (2010) 1680.
- [4] T.S. Narayanan, I.S. Park, M.H. Lee, *Prog. Mater. Sci.*, 60 (2014) 1.
- [5] C.-E. Barchiche, E. Rocca, C. Juers, J. Hazan, J. Steinmetz, *Electrochim. Acta*, 53 (2007) 417.
- [6] H.M. Wong, K.W. Yeung, K.O. Lam, V. Tam, P.K. Chu, K.D. Luk, K.M. Cheung, *Biomaterials*, 31 (2010) 2084.
- [7] A. Abdal-hay, N.A. Barakat, J.K. Lim, *Colloids Surf. A Physicochem. Eng. Asp.*, 420 (2013) 37.
- [8] J. Degner, F. Singer, L. Cordero, A.R. Boccaccini, S. Virtanen, *Appl. Surf. Sci.*, 282 (2013) 264.
- [9] P. Rosemann, J. Schmidt, A. Heyn, *Mater. Corros.*, 64 (2013) 714.
- [10] J. Wang, Y. He, M.F. Maitz, B. Collins, K. Xiong, L. Guo, Y. Yun, G. Wan, N. Huang, *Acta Biomater.*, 9 (2013) 8678.
- [11] E. Wittchow, N. Adden, J. Riedmueller, C. Savard, R. Waksman, M. Braune, *EuroIntervention*, 8 (2013) 1441.
- [12] M. Haude, R. Erbel, P. Erne, S. Verheye, H. Degen, D. Böse, P. Vermeersch, I. Wijnbergen, N. Weissman, F. Prati, *Lancet*, 381 (2013) 836.
- [13] L.B. Koh, I. Rodriguez, S.S. Venkatraman, *Biomaterials*, 31 (2010) 1533.
- [14] L.B. Koh, I. Rodriguez, S.S. Venkatraman, *Acta Biomater.*, 5 (2009) 3411.
- [15] C.K. Hashi, N. Derugin, R.R.R. Janairo, R. Lee, D. Schultz, J. Lotz, S. Li, *Arterioscler. Thromb. Vasc. Biol.*, 30 (2010) 1621.
- [16] X. Ma, T. Wu, M.P. Robich, *Interv. Cardiol.* , 4 (2012) 73.
- [17] Y. Lee, J. Kwon, G. Khang, D. Lee, *Tissue Eng. Part A*, 18 (2012) 1967.

- [18] L. Kong, W. Liu, G. Yan, Q. Li, H. Yang, F. Yu, H. Song, *Int. J. Clin. Exp. Med.*, 7 (2014) 5317.
- [19] F. Jung, C. Wischke, A. Lendlein, *MRS Bull.*, 35 (2010) 607.
- [20] Y. Hong, J. Guan, K.L. Fujimoto, R. Hashizume, A.L. Pelinescu, W.R. Wagner, *Biomaterials*, 31 (2010) 4249.
- [21] R. Hashizume, Y. Hong, K. Takanari, K.L. Fujimoto, K. Tobita, W.R. Wagner, *Biomaterials*, 34 (2013) 7353.
- [22] J. Guan, M.S. Sacks, E.J. Beckman, W.R. Wagner, *J. Biomed. Mater. Res.*, 61 (2002) 493.
- [23] J. Wang, V. Giridharan, V. Shanov, Z. Xu, B. Collins, L. White, Y. Jang, J. Sankar, N. Huang, Y. Yun, *Acta Biomater.*, 10 (2014) 5213.
- [24] V.N. Shanov, P. Roy-Chaudhury, M.J. Schulz, B. Campos-Naciff, Y. Wang, *PCT/US 1332374 2013*, 2013.
- [25] S.-H. Ye, Y.-S. Jang, Y.-H. Yun, V. Shankarraman, J.R. Woolley, Y. Hong, L.J. Gamble, K. Ishihara, W.R. Wagner, *Langmuir*, 29 (2013) 8320.
- [26] Y. Tamada, E.A. Kulik, Y. Ikada, *Biomaterials*, 16 (1995) 259.
- [27] Q. Cai, G. Shi, J. Bei, S. Wang, *Biomaterials*, 24 (2003) 629.
- [28] T. Yoshioka, N. Kawazoe, T. Tateishi, G. Chen, *Biomaterials*, 29 (2008) 3438.
- [29] Y. Xin, K. Huo, H. Tao, G. Tang, P.K. Chu, *Acta Biomater.*, 4 (2008) 2008.
- [30] J. Daemen, P.W. Serruys, *Circulation*, 116 (2007) 316.
- [31] I. Sheiban, G. Villata, M. Bollati, D. Sillano, M. Lotrionte, G. Biondi-Zoccai, *Vasc. Health Risk Manag.*, 4 (2008) 31.
- [32] A.S. Puranik, E.R. Dawson, N.A. Peppas, *Int. J. Pharm.*, 441 (2013) 665.
- [33] [http://www.fiercemedicaldevices.com/story/boston-scientifics-synergy-becomes-first-partially-bioabsorbable-stent-gain/2015-10-05?utm\\_campaign=+SocialMedia](http://www.fiercemedicaldevices.com/story/boston-scientifics-synergy-becomes-first-partially-bioabsorbable-stent-gain/2015-10-05?utm_campaign=+SocialMedia).
- [34] J.A. Ormiston, P.W. Serruys, *Circ. Cardiovasc. Interv.*, 2 (2009) 255.
- [35] H. Tamai, K. Igaki, E. Kyo, K. Kosuga, A. Kawashima, S. Matsui, H. Komori, T. Tsuji, S. Motohara, H. Uehata, *Circulation*, 102 (2000) 399.
- [36] S.G. Ellis, D.J. Kereiakes, D.C. Metzger, R.P. Caputo, D.G. Rizik, P.S. Teirstein, M.R. Litt, A. Kini, A. Kabour, S.O. Marx, *N. Engl. J. Med.*, 373 (2015) 1905.
- [37] J. Iqbal, Y. Onuma, J. Ormiston, A. Abizaid, R. Waksman, P. Serruys, *Eur. Heart J.*, 35 (2014) 765.
- [38] M. Haude, H. Ince, A. Abizaid, R. Toelg, P.A. Lemos, C. von Birgelen, E.H. Christiansen, W. Wijns, F.-J. Neumann, C. Kaiser, *Lancet*, 387 (2016) 31.
- [39] S. Ramcharitar, P.W. Serruys, *Am. J. Cardiovasc. Drugs*, 8 (2008) 305.
- [40] D. Pierson, J. Edick, A. Tauscher, E. Pokorney, P. Bowen, J. Gelbaugh, J. Stinson, H. Getty, C.H. Lee, J. Drelich, *J. Biomed. Mater. Res. Part B Appl. Biomater.*, 100 (2012) 58.
- [41] P.K. Bowen, J. Drelich, J. Goldman, *Adv. Mater.*, 25 (2013) 2577.
- [42] P.K. Bowen, R.J. Guillory, E.R. Shearier, J.-M. Seitz, J. Drelich, M. Bocks, F. Zhao, J. Goldman, *Mater. Sci. Eng. C*, 56 (2015) 467.
- [43] Y. Chen, Y. Song, S. Zhang, J. Li, C. Zhao, X. Zhang, *Biomed. Mater.*, 6 (2011) 025005.
- [44] P. In Pyo Park, S. Jonnalagadda, *J. Appl. Polym. Sci.*, 100 (2006) 1983.
- [45] W. Ferrando, *J. Mater. Eng.*, 11 (1989) 299.
- [46] I. Johnson, H. Liu, *PLoS One*, 8 (2013) e65603.
- [47] H. Wang, Z. Shi, *J. Biomed. Mater. Res. Part B Appl. Biomater.*, 98 (2011) 203.
- [48] Y. Song, D. Shan, R. Chen, F. Zhang, E.-H. Han, *Mater. Sci. Eng. C Mater. Biol. Appl.*, 29 (2009) 1039.
- [49] D. Xue, Y. Yun, Z. Tan, Z. Dong, M.J. Schulz, *J. Mater. Sci. Technol.*, 28 (2012) 261.
- [50] J. Walker, S. Shadanbaz, N.T. Kirkland, E. Stace, T. Woodfield, M.P. Staiger, G.J. Dias, *J. Biomed. Mater. Res. Part B Appl. Biomater.*, 100 (2012) 1134.
- [51] C. Liu, Y. Xin, X. Tian, P.K. Chu, *J. Mater. Res.*, 22 (2007) 1806.

- [52] X. Gu, Y. Zheng, Y. Cheng, S. Zhong, T. Xi, *Biomaterials*, 30 (2009) 484.
- [53] D.W. Wang, Y. Cao, H. Qiu, Z.G. Bi, *J. Biomed. Mater. Res. A.*, 99 (2011) 166.
- [54] Y. Hong, S.-H. Ye, A.L. Pelinescu, W.R. Wagner, *Biomacromolecules*, 13 (2012) 3686.
- [55] J. Fang, S.-H. Ye, V. Shankarraman, Y. Huang, X. Mo, W.R. Wagner, *Acta Biomater.*, 10 (2014) 4639.
- [56] M. Houchin, E. Topp, *J. Appl. Polym. Sci.*, 114 (2009) 2848.
- [57] A.V. Finn, M. Joner, G. Nakazawa, F. Kolodgie, J. Newell, M.C. John, H.K. Gold, R. Virmani, *Circulation*, 115 (2007) 2435.
- [58] Y. Farhatnia, A. Tan, A. Motiwala, B.G. Cousins, A.M. Seifalian, *Biotechnol. Adv.*, 31 (2013) 524.
- [59] R. Blindt, F. Vogt, I. Astafieva, C. Fach, M. Hristov, N. Krott, B. Seitz, A. Kapurniotu, C. Kwok, M. Dewor, *J. Am. Coll. Cardiol.*, 47 (2006) 1786.
- [60] Q. Lin, X. Ding, F. Qiu, X. Song, G. Fu, J. Ji, *Biomaterials*, 31 (2010) 4017.
- [61] C.K. Poh, Z. Shi, T.Y. Lim, K.G. Neoh, W. Wang, *Biomaterials*, 31 (2010) 1578.
- [62] L.J. Taite, P. Yang, H.W. Jun, J.L. West, *J. Biomed. Mater. Res. Part B Appl. Biomater.*, 84 (2008) 108.
- [63] J. Yang, Y. Zeng, C. Zhang, Y.-X. Chen, Z. Yang, Y. Li, X. Leng, D. Kong, X.-Q. Wei, H.-F. Sun, *Biomaterials*, 34 (2013) 1635.

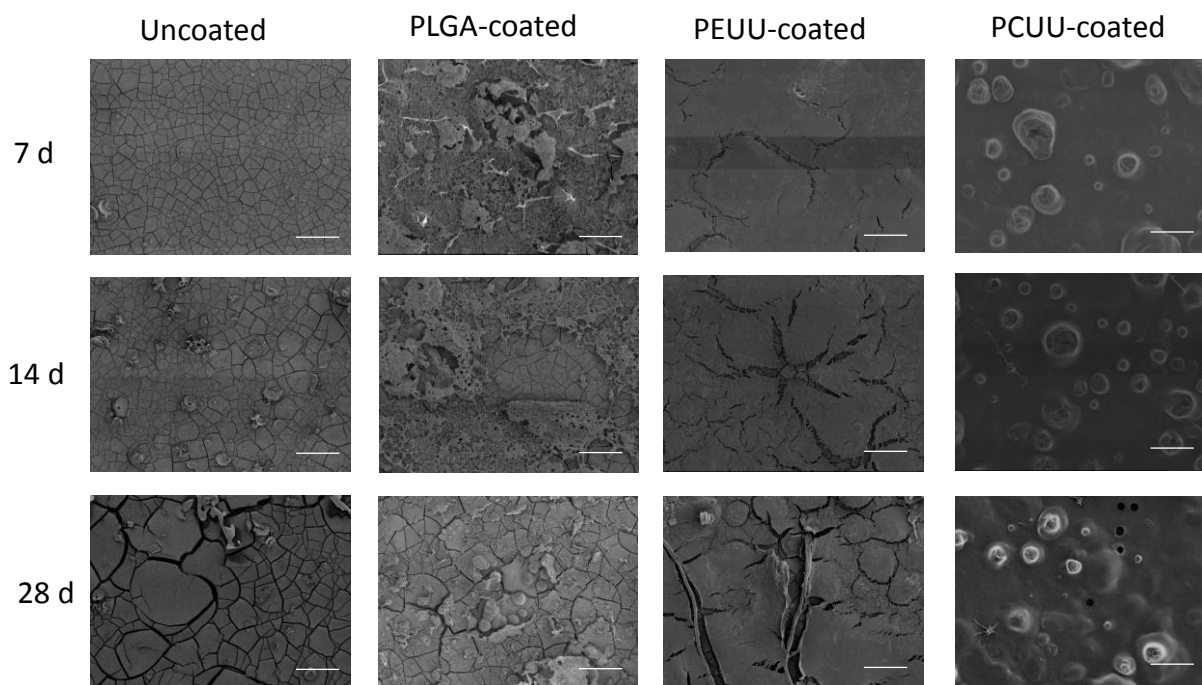


**Fig. 1.** Surface morphologies of AZ31 coated and uncoated samples incubated in DMEM (10% FBS, 1% P/S)+100 U/ml lipase solution at 37°C for 7, 14, and 28 days with mixing. Medium was changed every other day. Scale bars: 100 μm.



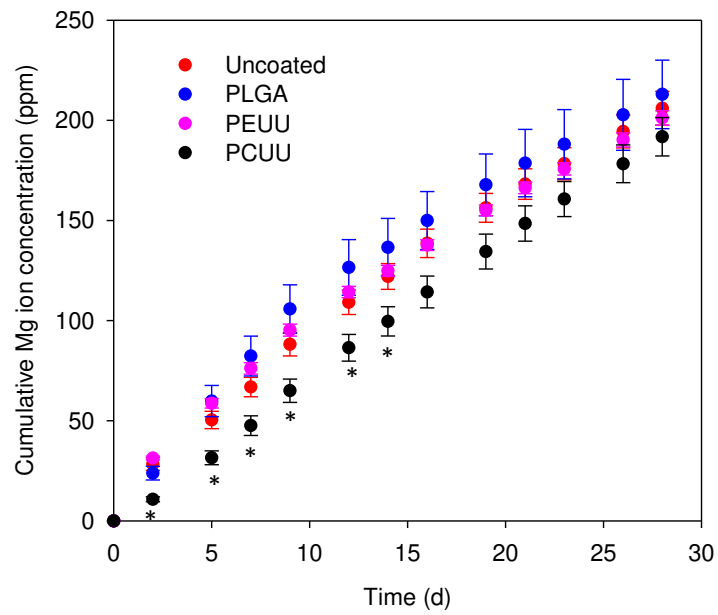


**Fig. 2.** Cumulative magnesium ion concentration in extracted incubation media for AZ31 coated and uncoated samples, measured by inductively coupled plasma atomic emission spectroscopy (ICP-AES); \* $p < 0.05$ .

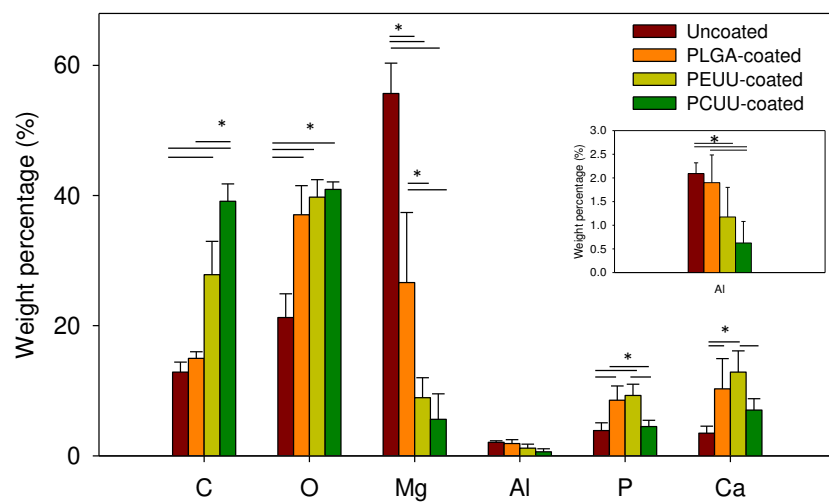


**Fig. 3.** Weight percentages for atoms shown on uncoated and coated AZ31 plates following 21 days degradation tests by energy-dispersive X-ray spectroscopy.\* $p < 0.05$ .

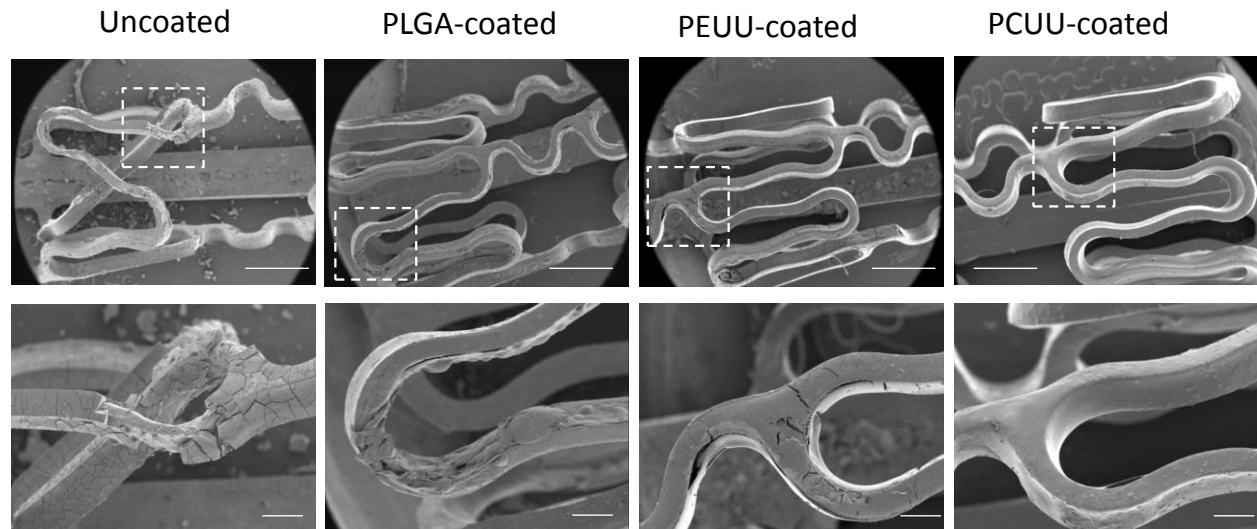


**Fig. 4.** SEM images of corrosion regions on AZ31 stents under the flow-induced shear stress values of 0.07Pa for 3 days in DMEM (10% FBS, 1% P/S)+100 U/ml lipase solution at 37°C . Images in the bottom row are the enlarged images of the white dashed box in images in the top row. Scale bar = 1 mm top row; 200  $\mu$ m bottom row.

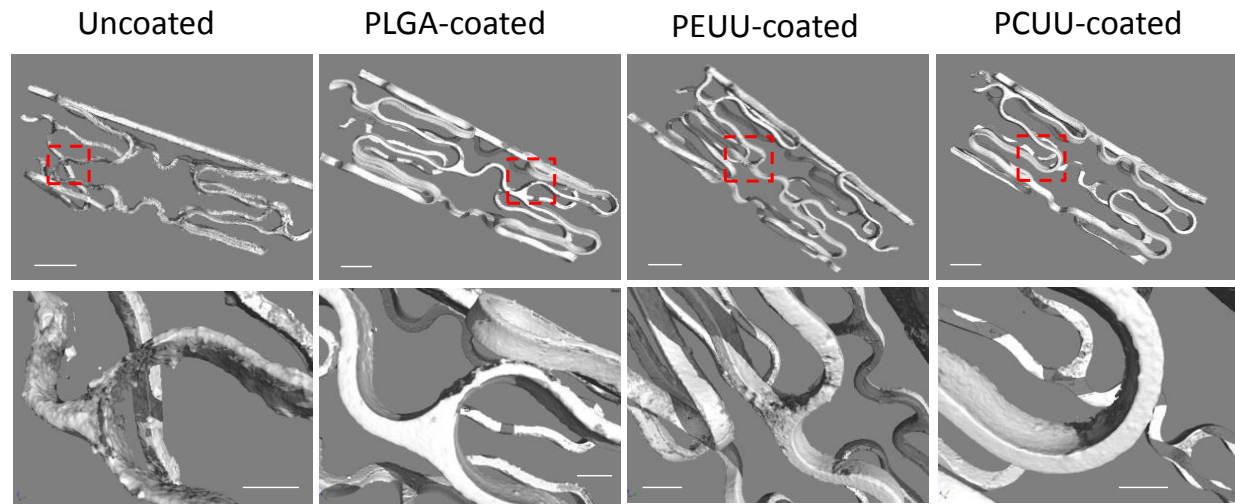


**Fig. 5.** Reconstructions of X-ray micro-CT 3-D images of stents under dynamic conditions in DMEM (10% FBS, 1% P/S)+100 U/ml lipase solution at 37°C for 3 days. Images in the bottom row are the enlarged images of the red dashed box in images in the top row. Scale bar = 1 mm top row; 0.5 mm bottom row.

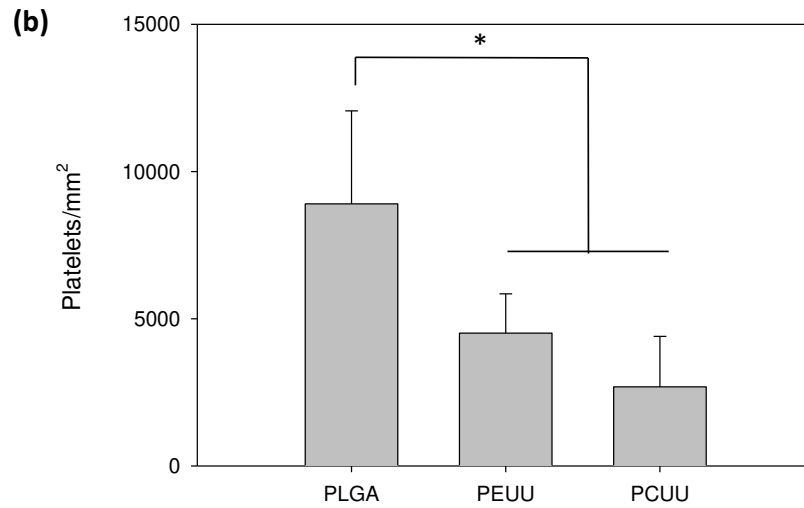
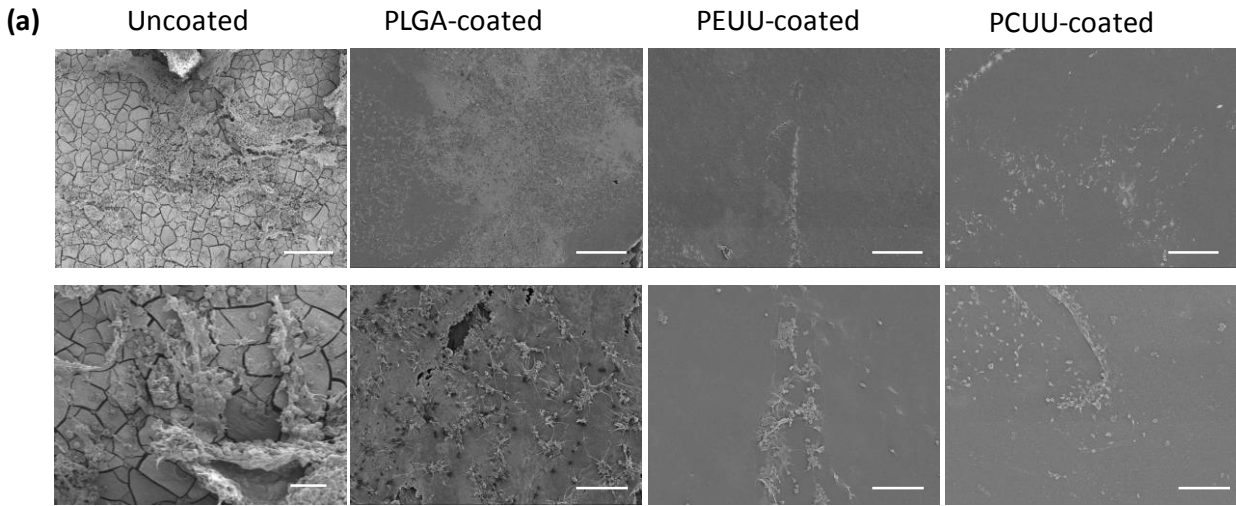


**Fig. 6. (a)** Electron micrographs of AZ31 samples after contact with ovine blood for 2 h. Images in the bottom row are the enlarged images of the red dashed box in images in the top row. Scale bar = 100  $\mu\text{m}$  top row; 20  $\mu\text{m}$  bottom row. **(b)** Platelet deposition on coated AZ31 plates as quantified by LDH assay after 2 h of blood contact at 37°C. \* $p < 0.05$ .

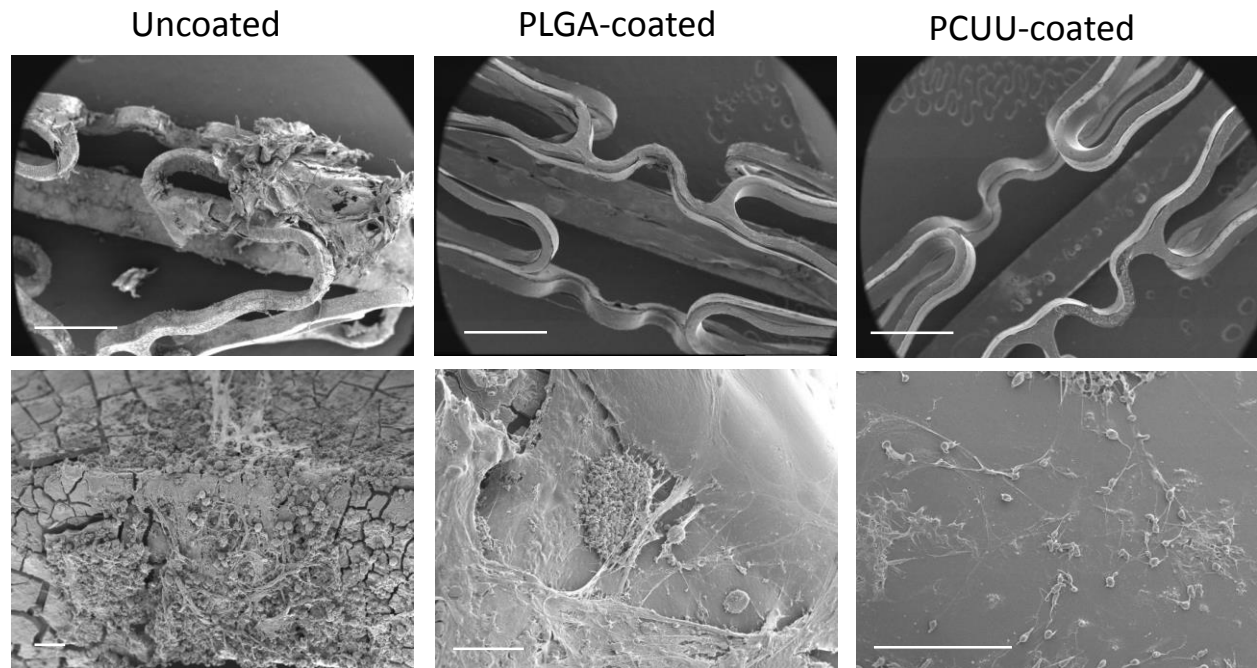


**Fig. 7.** Electron micrographs of AZ31 stents after contact with ovine blood for 2 h. Images in the bottom row are the enlarged images of images in the top row. Scale bar = 1 mm top row; 20  $\mu$ m bottom row.

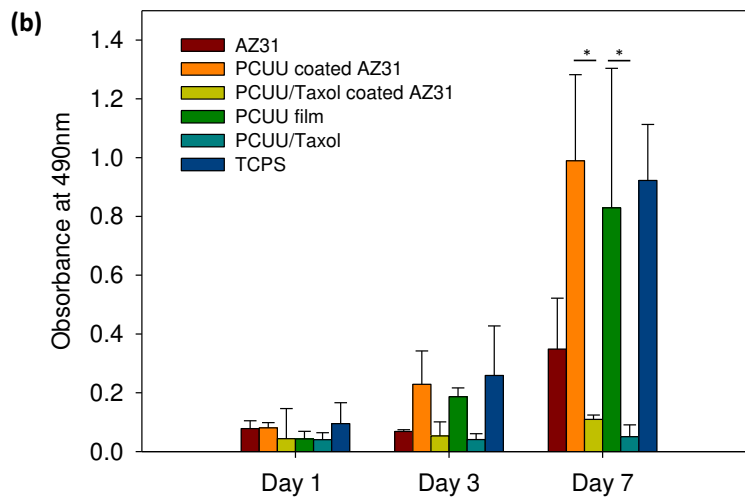
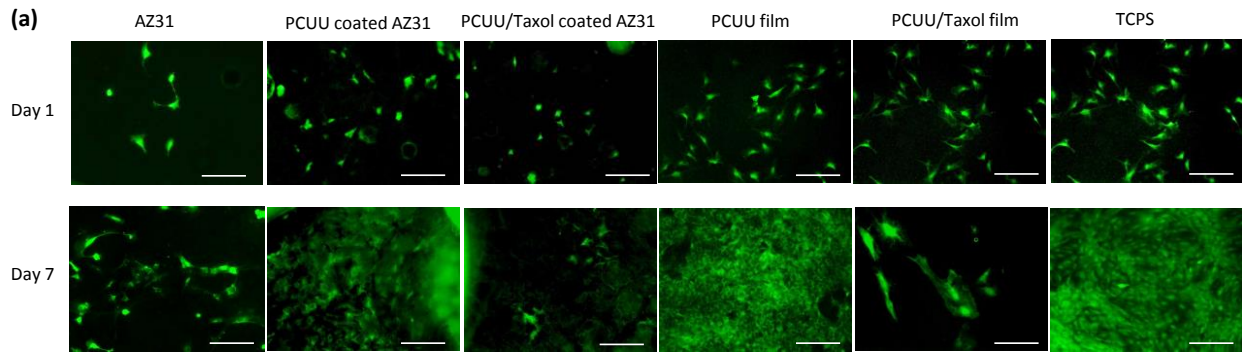


**Fig. 8. (a)** Culture of rSMCs on control and modified surfaces indicates the bioactivity of released paclitaxel following live/dead staining. Scale bars: 200  $\mu\text{m}$ . **(b)** Metabolic index using the MTS assay of rSMCs cultured on different samples. TCPS was utilized as a control; \* $p < 0.05$

